EVALUATING EFFECTIVE REACTION RATES OF KINETICALLY DRIVEN SOLUTES IN LARGE-SCALE, STATISTICALLY ANISOTROPIC MEDIA: IMPLICATIONS OF PORE SCALE MIXING AND PREFERENTIAL FLOW PATHWAYS AT THE FIELD SCALE

Erica R. Siirila[*] and Reed M. Maxwell[†]

Colorado School of Mines
Department of Geology and Geological Engineering
1500 Illinois St., Golden, CO 80401 USA
[*] e-mail: esiirila@mymail.mines.edu, web page: http:// http://inside.mines.edu/~esiirila/
[†] e-mail: rmaxwell@mines.edu, web page: http://inside.mines.edu/~rmaxwell/

Key words: stochastic, groundwater contamination, dispersion, kinetics

Summary. The role of high and low hydraulic conductivity (K) regions in heterogeneous flow fields with varying degrees of stratification and the subsequent effect of rate-dependent geochemical reactions is investigated. An example contamination scenario is used to to investigate potential impacts of kinetic sorption and local dispersion on plume migration and channeling. In this study, kinetic sorption is simulated with finely resolved, large-scale domains to identify geo-hydrologic conditions where solute reactions are either rate limited (non-reactive), in equilibrium (linear equilibrium assumption, LEA, is appropriate), or are sensitive to time-dependent kinetic reaction rates. By utilizing stochastic ensembles, local and effective equilibrium conditions are examined, in addition to potential interplay between multiple parameters (i.e. positive or negative feedbacks). In particular, the effect of preferential flow pathways and solute mixing at the field-scale (marcrodispersion) and sub-grid (local dispersion) is examined for varying degrees of stratification and regional groundwater velocities. Results show effective reaction rates of kinetic ensembles with the inclusion of local dispersion yield dis-equilibrium transport, even for averaged (or global) Damköholer numbers associated with equilibrium transport. Resulting solute behavior includes an additive tailing effect of the plume, and a retarded peak time. This discrepancy between kinetic and LEA ensembles is augmented in highly anisotropic media. Comparisons with non-reactive solutes simulated with the inclusion of local dispersion exhibit not only an increase in plume spreading but also effective plume retardation.

1 INTRODUCTION

In this analysis, feedbacks between pore scale mixing (local-scale dispersion, LD), large scale mixing (macrodispersion), and small-scale reactions are analyzed. The numerical framework utilized in this study is stochastic, where concentrations in a three-dimensional heterogeneous media are assessed probabilistically. Specifically we investigate the effect of kinetically sorbing

solutes in highly-stratified aquifers, a topic addressed in the early literature for more simplified heterogeneous domains[1-4]. Here we use stratified domains to assess realistic far-field groundwater contamination scenarios where variations in sedimentology and stratigraphy are dominant factors in determining contaminant flow and transport. Stratified aquifers are often associated with non-ergodic transport[5], or when the ensemble statistics do not coincide with the corresponding spatial averages calculated over a single realization[6]. The stratified aquifer is also of interest because (1) the stratigraphy of many natural formations are highly anisotropic e.g. see Table 2.1 of Rubin, 2003[7] and (2) inter-connected pathways are much more prevalent, where channeling of solutes through areas of higher hydraulic conductivity effectively decreases the overall effect of macrodispersion[8]. The results shown here have implications in a wide range of groundwater contamination scenarios involving reactive solutes, including but not limited to, acid-mine drainage, CO_2 leakage from Carbon Capture and Storage (CCS), other forms of underground waste storage, agricultural and urban run-off, disposal of industrial wastewater, etc.

2 METHODOLOGY

In the present analysis, a case-study is used to simulate an example contamination scenario involving mobilized arsenic (see Table 1 for parameter inputs and domain setup). Multiple ensembles (each composed of 200 realizations) of large-extent, highly-resolved, regional-scale aquifers are simulated to account for subsurface uncertainty with flow and transport codes through the use of parallel high performance computing. Far-field aquifer flow is simulated using the parallel, three-dimensional groundwater model ParFlow,[9-11].

Both the validity and predictability of LEA is investigated by stochastically simulating ensembles of both linear and kinetic sorption scenarios with the Lagrangian particle tracking model, SLIM-FAST[12-14]. Non-reactive (i.e. tracer), LEA, and first-order kinetic particle simulations are conducted. LEA simulations utilize the partition coefficient (K_D) [L kg^{-1}], defined as the slope of sorption isotherm relating the aqueous concentration in solution (C) [mg kg^{-1}] is to the sorbed concentration in the solid phase (C^*) [mg m^{-3}]. Kinetic simulations utilize time dependent forward (k_f) [L d^{-1}] and reverse (k_r) [kg d^{-1}] rates with an equivalent ratio to the partition coefficient:

$$K_D = \frac{k_f}{k_r} = \frac{C^*}{C}$$

(1)

All sorption parameters (K_D, k_f, k_r) are constant in space and time. Traditionally, the use of the dimensionless Damköhler number has been used as a predictor to distinguish when LEA or kinetic modeling is appropriate e.g.[15, 16-20]. We define a global estimate of the Damköhler number as:

$$Da_{Global} = \frac{k_f * \Delta x}{v}$$

(2)

Following the aforementioned studies examining Damköhler numbers, large Da values, typically over 10.0 [-], suggest that the LEA is appropriate because the contaminant will have sufficient time to sorb to the porous media (i.e. sorption reaction time is small relative to the groundwater

Parameter	Value	Units
Domain Size (x_d, y_d, z_d)	~ (4000 x 1000 x 100)	[m]
Cell discretization (Δx, Δy, Δz)	(3.0 x 3.0 x 0.3)	[m]
Number of cells (nx, ny, nz)	(1333 x 333 x 333)	-
Location of source (x, y, z)	(500.0, 500.0, 30.0)	[m]
$v = 0.01$ [m d^{-1}]	$\Delta h = 0.317$	[m]
Number of particles	300,000	-
Geometric mean of Y	$K_{G,\,Y} = 52$	[m d^{-1}]
Standard deviation of Y	$\sigma_Y = 1.9$	-
Porosity	$\theta = 0.33$	-
Well pumping rates	$Q_w = 500$	[m^3 d^{-1}]
Well screen length	$s_w = 20$	[m]
Well locations	$x_w = 3500$, $z = 75$	[m]
	$y_w = (800, 600, 400, 200)$	[m]
Anisotropy ratios		
$\varepsilon = 0.1$ [-]	$\lambda_h = 15.0$, $\lambda_v = 1.5$	[m]
$\varepsilon = 0.006$ [-]	$\lambda_h = 250.0$, $\lambda_v = 1.5$	[m]
Sorption scenarios		
LEA, partition coefficient	$K_D = 25$	[L kg^{-1}]
Kin1, forward and reverse rates	$k_f = 2.88$, $k_r = 0.115$	[L d^{-1}]
Kin2, forward and reverse rates	$k_f = 28.80$, $k_r = 1.150$	[kg d^{-1}]
Local dispersion scenarios		
$Pe = \infty$ [-]	$\alpha_L = 0.0$, $\alpha_T = 0.0$	[m]
$Pe = 1.5 \times 10^4$ [-]	**For $\lambda_h = 15.0$:**	
	$\alpha_L = 0.001$, $\alpha_T = 0.0001$	[m]
$Pe = 2.5 \times 10^5$ [-]	**For $\lambda_h = 250.0$:**	
	$\alpha_L = 0.001$, $\alpha_T = 0.0001$	[m]

Table 1 : Domain setup and parameter inputs.

velocity). Likewise small *Da* values, typically below 1.0 [-], suggest that the contaminant will not have sufficient time to sorb to the porous media; intermediate *Da* values are rate limited, and forward and reverse kinetic modeling is needed.

Local (or sub-grid) dispersion (LD) has also been linked to sensitivity in higher order moments (i.e. mean solute point flux and concentration variances) [21-24]. This increase in dispersion is quantified in terms of displacement by the non-dimensional Péclet number (*Pe*) [-]:

$$Pe = \frac{v_x \lambda_{x=y}}{D_L} = \frac{\lambda_{x=y}}{\alpha_L}$$

(3)

LD has also been found to be especially significant in three-dimensional stratified aquifers,

where given high *Pe* numbers and low ε, the neglect of LD may yield in-accurate results[22]. Fiori[25] also had a similar finding for $\varepsilon \leq 0.1$, where both studies analyzed *Pe* numbers up to $O(10^3 - 10^4)$. Combinations of infinite ($Pe = \infty$) and finite ($Pe \neq \infty$) Péclet numbers of $O(10^4 - 10^5)$ at low anisotropy ratios ($\varepsilon \leq 0.1$) are simulated in this case study to examine aquifer settings where sedimentology and stratigraphy are controlling factors in flow and transport. Combinations of high *Pe* and low ε have been briefly investigated in the literature e.g. [26].

For each sorption scenario (LEA versus kinetic), effective retardation is expressed relative to t_{pk} and C_{pk} of the corresponding tracer simulation of that realization, where:

$$R_{eff,LEA} = \frac{t_{pk,LEA}}{t_{pk,tracer}} \qquad R_{eff,kin} = \frac{t_{pk,kin}}{t_{pk,tracer}} \tag{4}$$

This essentially uses the conservative tracer simulations as a control by holding the parameters ε, v, and *Pe*, constant and isolating the effect of the sorption scenario alone. Equations 4 are based on the results of the numerical simulations and describe the effective retardation of the overall plume. Because of the relationship imposed between the ratio k_f/k_r and K_D (see Equation 1), if LEA is an appropriate assumption, $R_{eff,LEA}$ is equivalent to $R_{eff,kin}$, regardless of the hydrologic domain or the transport parameters.

To investigate the effect of LD, the differences between non-reactive breakthroughs are compared for $Pe = \infty$ and $Pe \neq \infty$ scenarios through the effective retardation of dispersion, $R_{eff,Disp}$:

$$R_{eff,Disp} = \frac{\left[t_{pk,tracer}\right]_{Pe \neq \infty}}{\left[t_{pk,tracer}\right]_{Pe = \infty}} \tag{5}$$

To isolate the effect of LD alone, Equation 5 is calculated for the tracer simulations (i.e. excludes the sorption scenario). This metric holds the parameters ε, and v constant while isolating the effect of *Pe* alone.

3   RESULTS AND DISCUSSION

Figure 1 shows a scatter plot (4 ensembles, 200 realizations each) of effective kinetic retardations ($R_{eff,Kin1}$) versus normalized peak tracer concentrations ($C_{pk}/C_{pk,tracer}$) with infinite *Pe* (Figure 1 a) and finite *Pe* (Figure 1 b). The crossbar intersection at $R_{eff} = 26$ [-] and $C_{pk,Kin1}/C_{pk,tracer} \approx 0.038$ [-] corresponds to the expected solute retardation if equilibrium is an appropriate assumption. For the scenarios shown here, Da_{Global} is greater than 10, and well into the equilibrium regime. Results for *Kin1* simulations are shown here; LEA ensembles (not shown here) are centered at the crossbar intersection, as expected.

Kin1 ensembles are not centered at the crossbar intersection but rather are centered between $R_{eff} = 40 - 70$[-] with corresponding $C_{pk,Kin1}/C_{pk,tracer}$ values less than 0.038. In other words, the majority of kinetic realizations yield a more retarded peak arrival time and concentration when compared to the LEA realizations, even though the expected retardations are equivalent. This result demonstrates the influence of the rate dependence associated with kinetic sorption, and how it potentially impacts both peak concentration and peak times.
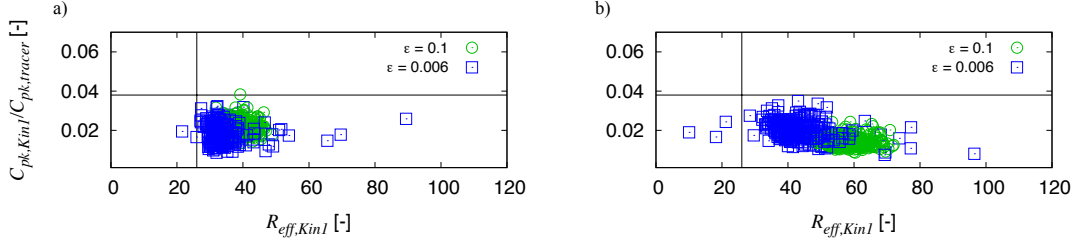
4

Figure 1. *Kin1* effective retardation ratios versus normalized peak concentrations for both ε, for each realization within infinite *Pe* (a) and finite *Pe* (b) ensembles.

Differences in stratification are also apparent in Figure 1, where smaller ε demonstrate less variance in R_{eff} and greater ε demonstrate more variance in R_{eff}. In other words, the normalized arrival times for more stratified domains are consistent in contrast to the less consistent arrival times with the less stratified domain. This effect can also be attributed to channeling and preferential flow pathways in the stratified domain.

Secondly, while the majority of the scatter is shifted towards greater R_{eff} values (i.e. more retarded peak times), several realizations show much smaller R_{eff} values, and therefore very fast arrival times. This is especially true for finite *Pe* ensembles (right panel of Figure 1). It is also important to note the centered value of R_{eff} for finite *Pe*, *Kin1* ensembles is nearly double that of LEA ensembles. This feedback between kinetic sorption and local dispersion, (and the resulting faster peak times) can be explained by the schematic in Figure 2.

Here the induced cell-based mixing creates particle jumps from interconnected high K regions into regions of low K and vice versa. We speculate that the effect of the time dependence associated with kinetic sorption into and out of solution is magnified, yielding solute behavior unlike that of equilibrium simulations. This process is illustrated at the high-low K interface in the schematic representation shown in Figure 2 for a) LEA sorption and b-c) two possible kinetic sorption scenarios. This schematic highlights the process of particle retardation when LD forces the particle into neighboring high or low K zones. Particle movement at the time of LD (t_{Disp}, bottom panel of Figure 2) is indicated by particle locations 0-10, where equal time has elapsed between each incrementing particle location. Solid-end cap lines indicate the magnitude of particle displacement whereas vector lines indicate the magnitude of the groundwater velocity. The magnitude of particle velocity is shown in the panel labeled $v_{particle}$. Because LEA is assumed in Figure 2a, the $v_{particle}$ is retarded by a factor of R regardless of if the particle is located in a high or low K zone (i.e. v/R, where R is the expected retardation). When kinetically controlled particles (Figure 2 b-c), are located within a low K zone, $v_{particle}$ is analogously equivalent to v/R. The assumption here is that v is much slower in low K zones than in high K zones, and is favorable to equilibrium conditions (akin to a high Da). When kinetically-controlled particles are located within a high K zone, $v_{particle}$ is equivalent to v retarded by a factor of $R_{eff,kin}$ (i.e. $v/R_{eff,kin}$, see Equation 4). Depending on the actual magnitude of v in the high K zone, this regime is analogous to low and intermediate Da. An example of an intermediate (kinetic dependent) Da is shown in Figure 2b, where $R_{eff,kin} < R$, and the particle displacement
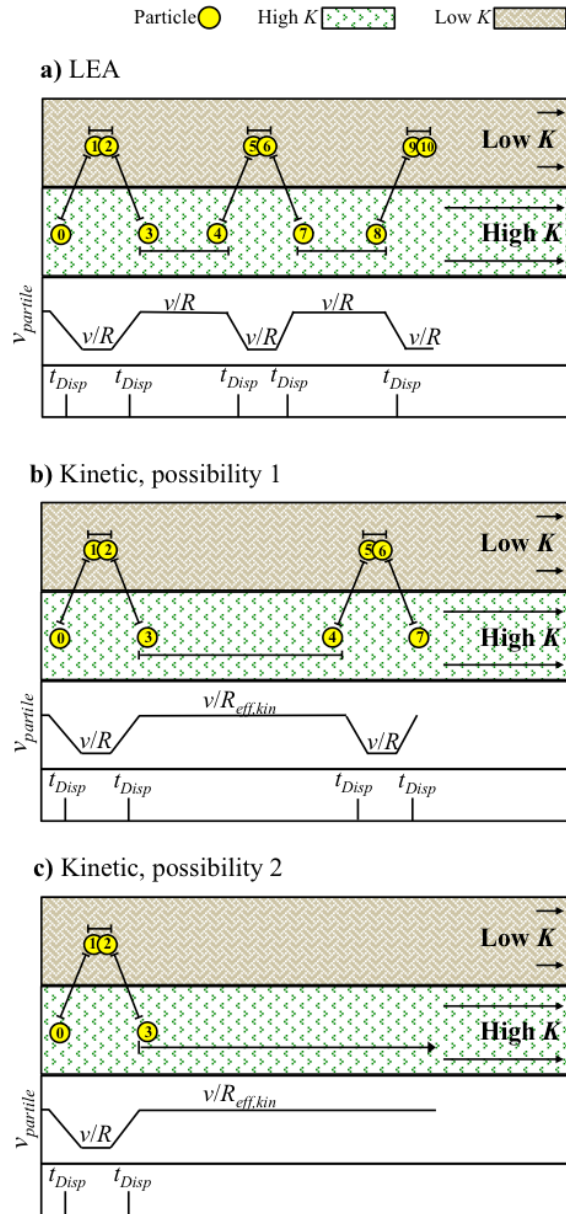
5

Figure 2. Schematic high-low K interface given LD for a) LEA sorption and b-c) two kinetic sorption scenarios.

between particle locations 3 and 4 is larger in the kinetic case. The extreme case of very low Da is depicted in Figure 2 c, where the magnitude of v in the high K zone is very high in relationship to the rate of the reaction, and $R_{eff,kin} << R$. As $R_{eff,kin}$ approaches unity, the particle is less retarded and behaves similar to a tracer. This is illustrated by the large particle displacement between locations 3 and 4. Our results, along with the conceptual model, indicate that there is an

additive process involving kinetic sorption and LD that include: 1) particle retardation similar to LEA in low K zones where low v regimes are conducive to equilibrium conditions, 2) lower particle retardation in high K zones via less reaction time in high v regimes, 3) shorter particle displacement in low K zones and longer particle displacements in high K zones, and 4) a higher frequency of t_{Disp} in LEA scenarios compared to kinetic scenarios.

The effective retardation of dispersion, $R_{eff,Disp}$, is used to isolate the effect of LD through the use of Equation 4. This metric is performed on tracer simulations only in order to separate the effect of the sorption scenario. Figure 3 shows $R_{eff,Disp}$ versus $[C_{pk}]_{Pe\neq\infty} / [C_{pk}]_{Pe=\infty}$ at both ε (see sub-plots). The driver in $R_{eff,Disp}$ behavior is the difference in ε. The less stratified domain ($\varepsilon = 0.1$) exhibits little difference between finite and infinite Pe, as shown by a clustered $R_{eff,Disp}$ near unity ($R_{eff,Disp} = 1$, $C_{pk}/C_0 = 1$). In contrast, the stratified domain ($\varepsilon = 0.006$) exhibits scatter far from the unity point. A majority of this scatter (> 50% of points) falls within quadrants II and IV in Figure 3 a-c. Quadrant II reflects when: 1. $(t_{pk,Pe \neq \infty}) \leq (t_{pk,Pe = \infty})$ and 2. $(C_{pk,Pe \neq \infty}) \geq (C_{pk,Pe = \infty})$. In other words, when the inclusion of LD yields a faster peak time and a higher concentration. Quadrant IV reflects when: 1. $(t_{pk,Pe \neq \infty}) \geq (t_{pk,Pe = \infty})$ and 2. $(C_{pk,Pe \neq \infty}) \leq (C_{pk,Pe = \infty})$. Or, when the inclusion of LD yields a slower peak time and a lower concentration.
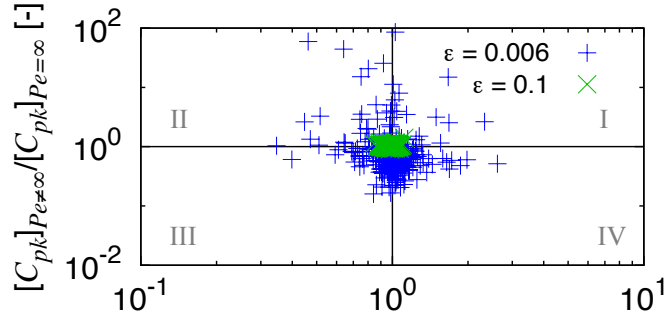

Figure 3. Effective retardation of dispersion versus normalized peak concentration for varying ε.

The $\varepsilon = 0.006$ scatter in quadrant II reflects when the inclusion of LD forces the contaminant from zones of low K into zones of higher K. Similarly, $\varepsilon = 0.006$ scatter in quadrant IV reflects movement from zones of high K into zones of lower K. This finding suggests the inclusion of LD (even on the mm scale) will cause either a retardation or acceleration of the plume. While other studies have shown the effect of LD affects higher order moments[21-24], to the best knowledge of the authors, the theory of LD as a catalyst of retardation of the first order moment has yet to be reported. This result regarding LD builds on the previous theories regarding diffusion suggested by LaBolle and co-authors[27, 28]. The effect of kinetic sorption is isolated from this result, and is therefore applicable (and has implications) in the theory of non-sorbing solutes as well.

4 CONCLUSIONS

The effects of kinetically sorbing solutes in stratified aquifers were studied to assess realistic

far-field groundwater contamination scenarios. An additive feedback, between LD and kinetic sorption was found to be a controlling process in simulating solute behavior by adding an effective tailing behavior as high as approximately 30 times that of a LEA solute without LD. This effect is controlled at the high-low K interface, where the induced cell-based mixing creates particle jumps from interconnected high K regions into regions of low K and vice versa. We also show parametric sensitivity to LD with the degree of aquifer stratification, where stratified aquifers show induced acceleration or retardation, and less stratified aquifers do not.

REFERENCES

[1] Valocchi, A.J., *Theoretical analysis of deviations from local equilibrium during sorbing solute transport through idealized stratified aquifers.* Journal of contaminant hydrology, 1988. **2**(3): p. 191-207.

[2] Valocchi, A.J., *Spatial moment analysis of the transport of kinetically adsorbing solutes through stratified aquifers.* Water Resour. Res., 1989. **25**(2): p. 273-279.

[3] Cvetkovic, V. and A. Shapiro, *Mass arrival of sorptive solute in heterogeneous porous media.* Water resources research, 1990. **26**(9): p. 2057-2067.

[4] Andričević, R. and E. Foufoula-Georgiou, *Modeling kinetic non-equilibrium using the first two moments of the residence time distribution.* Stochastic Hydrology and Hydraulics, 1991. **5**(2): p. 155-171.

[5] Sánchez-Vila, X. and J. Solís-Delfín, *Solute transport in heterogeneous media : The impact of anisotropy and non-ergodicity in risk assessment.* Stochastic Environmental Research and Risk Assessment, 1999. **13**(5): p. 365-379.

[6] Christakos, G., *Random field models in earth sciences*1992: Academic Press San Diego:.

[7] Rubin, Y., *Applied stochastic hydrogeology*2003: Oxford University Press, USA.

[8] Siirila, E.R., et al., *A quantitative methodology to assess the risks to human health from CO2 leakage into groundwater.* Advances in Water Resources, 2012. **36**(0): p. 146-164.

[9] Kollet, S.J. and R.M. Maxwell, *Integrated surface-groundwater flow modeling: A free-surface overland flow boundary condition in a parallel groundwater flow model.* Advances in Water Resources, 2006. **29**(7): p. 945-958

[10] Ashby, S. and R. Falgout, *A parallel multigrid preconditioned conjugate gradient algorithm for groundwater flow simulations.* Nuclear Science and Engineering, 1996. **124**(1): p. 145-159.

[11] Jones, J.E. and C.S. Woodward, *Newton-Krylov-multigrid solvers for large-scale, highly heterogeneous, variably saturated flow problems.* Advances in Water Resources, 2001. **24**(7): p. 763-774.

[12] Maxwell, R.M., *SLIM-FAST: A User's Manual V.4, GWMI.* 2010.

[13] Maxwell, R.M. and W.E. Kastenberg, *Stochastic environmental risk analysis: an integrated methodology for predicting cancer risk from contaminated groundwater.* Stochastic Environmental Research and Risk Assessment, 1999. **13**(1-2): p. 27-47.

[14] Maxwell, R.M., C. Welty, and R.W. Harvey, *Revisiting the Cape Cod Bacteria Injection*

Experiment Using a Stochastic Modeling Approach. Environmental Science & Technology, 2007. **41**(15): p. 5548-5558.

[15] Jennings, A.A., *Instantaneous equilibrium approximation analysis.* Journal of Hydraulic Engineering, 1984. **110**: p. 1700.

[16] Bahr, J.M. and J. Rubin, *Direct comparison of kinetic and local equilibrium formulations for solute transport affected by surface reactions.* Water resources research, 1987. **23**(3): p. 438-452.

[17] Espinoza, C. and A.J. Valocchi, *Stochastic analysis of one-dimensional transport of kinetically adsorbing solutes in chemically heterogeneous aquifers.* Water resources research, 1997. **33**(11): p. 2429-2445.

[18] Brusseau, M.L. and R. Srivastava, *Nonideal transport of reactive solutes in heterogeneous porous media 2. Quantitative analysis of the Borden natural-gradient field experiment.* Journal of contaminant hydrology, 1997. **28**(1-2): p. 115-155.

[19] Michalak, A.M. and P.K. Kitanidis, *Macroscopic behavior and random-walk particle tracking of kinetically sorbing solutes.* Water resources research, 2000. **36**(8): p. 2133-2146.

[20] Green, C.T., et al., *Mixing effects on apparent reaction rates and isotope fractionation during denitrification in a heterogeneous aquifer.* Water resources research, 2010. **46**(08).

[21] Dagan, G. and A. Fiori, *The influence of pore-scale dispersion on concentration statistical moments in transport through heterogeneous aquifers.* Water Resour. Res., 1997. **33**(7): p. 1595-1605.

[22] Bellin, A., A. Lawrence, and Y. Rubin, *Models of sub-grid variability in numerical simulations of solute transport in heterogeneous porous formations: three-dimensional flow and effect of pore-scale dispersion.* Stochastic Environmental Research and Risk Assessment, 2004. **18**(1): p. 31-38.

[23] Fiorotto, V. and E. Caroni, *Solute concentration statistics in heterogeneous aquifers for finite Peclet values.* Transport in porous media, 2002. **48**(3): p. 331-351.

[24] Fiori, A., et al., *A first-order analysis of solute flux statistics in aquifers: The combined effect of pore-scale dispersion, sampling, and linear sorption kinetics.* Water resources research, 2002. **38**(8): p. 1137.

[25] Fiori, A., *Finite Peclet Extensions of Dagan's Solutions to Transport in Anisotropic Heterogeneous Formations.* Water Resour. Res., 1996. **32**(1): p. 193-198.

[26] Indelman, P. and G. Dagan, *Solute transport in divergent radial flow through heterogeneous porous media.* Journal of Fluid Mechanics, 1999. **384**: p. 159-182.

[27] LaBolle, E.M., G.E. Fogg, and J.B. Eweis, *Diffusive fractionation of 3H and 3He in groundwater and its impact on groundwater age estimates.* Water resources research, 2006. **42**(7): p. W07202.

[28] LaBolle, E.M., et al., *Isotopic fractionation by diffusion in groundwater.* Water Resour. Res., 2008. **44**(7): p. W07405.